Geophysical Research Letters

RESEARCH LETTER
10.1029/2025GL120212

On the Role of Dynamical Uncertainties in the Spread of Arctic Ozone Recovery Projections

Samuel Benito-Barca[1], Marta Abalos[2], Natalia Calvo[2], Alvaro de la Cámara[2], Blanca Ayarzagüena[2], Gabriel Chiodo[1], Hideharu Akiyoshi[3], Fraser Dennison[4,5], Patrick Jöckel[6], Béatrice Josse[7], Doug Kinnison[8], Olaf Morgenstern[9,10,11], David Plummer[12], Timofei Sukhodolov[13], Yousuke Yamashita[3], and Shingo Watanabe[14,15]

[1]Instituto de Geociencias (IGEO), Consejo Superior de Investigaciones Científicas–Universidad Complutense de Madrid (CSIC–UCM), Madrid, Spain, [2]Departamento de Física de la Tierra y Astrofísica, Universidad Complutense de Madrid, Madrid, Spain, [3]Earth System Division, National Institute for Environmental Studies, Tsukuba, Japan, [4]CSIRO Environment, Aspendale, VIC, Australia, [5]School of Geography, Earth and Atmospheric Sciences, University of Melbourne, Parkville, VIC, Australia, [6]Institut für Physik der Atmosphäre, Deutsches Zentrum für Luft- und Raumfahrt (DLR), Oberpfaffenhofen, Germany, [7]Météo-France, CNRS, University Toulouse, CNRM, Toulouse, France, [8]National Center for Atmospheric Research, Boulder, CO, USA, [9]National Institute of Water and Atmospheric Research, Wellington, New Zealand, [10]School of Physical and Chemical Sciences, Canterbury University, Christchurch, New Zealand, [11]Now at Deutscher Wetterdienst, Offenbach, Germany, [12]Climate Research Division, Environment and Climate Change Canada, Montreal, QC, Canada, [13]Physikalisch-Meteorologisches Observatorium Davos/World Radiation Center, Davos, Switzerland, [14]Japan Agency for Marine-Earth Science and Technology (JAMSTEC), Yokohama, Japan, [15]Advanced Institute for Marine Ecosystem Change (WPI-AIMEC), Tohoku University, Sendai, Japan

Abstract Arctic ozone is projected to recover over the 21st century in compliance with the Montreal Protocol. Chemistry-climate models show a large spread in recovery rates and future changes in key dynamical features such as the polar vortex and the residual circulation. Here, we quantify the spread in Arctic ozone recovery explained by uncertainties in these dynamical changes, using simulations from the Chemistry-Climate Model Initiative, phases 1 and 2022. About 60% of the spread in projected ozone recovery is attributed to differences in polar vortex trends and about one-third to the intermodel spread in residual circulation trends. Ozone-depleting substances and greenhouse gas-driven global warming contribute similarly to the spread in ozone recovery, although uncertainties in dynamical trends primarily affect the warming component. While dynamical changes clearly separate the simulated ozone recovery among different models, the large variability in the Arctic stratosphere precludes establishing an observational constraint on future ozone recovery.

Plain Language Summary The recovery of Arctic ozone is expected throughout the 21st century thanks to the Montreal Protocol, an international treaty that phased out chemicals harming the ozone layer. However, there is significant uncertainty in how quickly this recovery will occur. Given that Arctic ozone is affected by the stratospheric dynamics, particularly the Brewer-Dobson Circulation (BDC) and the polar vortex, we study here how much of the uncertainty in ozone recovery is due to doubts in how the dynamics will change in the future. Our study shows that 60% of the differences in ozone recovery rates in model projections are due to uncertainty in the polar vortex evolution and 33% comes from uncertainty in the BDC acceleration. Both ozone-depleting substances and greenhouse gas-driven global warming affect recovery rates and its uncertainty. While dynamical changes clearly separate different models, the large year-to-year variability in the Arctic stratosphere makes it difficult to use present-day observations to assess which of the modeled projections are more credible, and thus, to accurately predict the timing of ozone recovery. Overall, our results highlight the need for a better understand of changes in stratospheric dynamics, which is critical for making reliable predictions about the ozone layer recovery.

Key Points:

- Seventy-five percent of the spread in Arctic ozone recovery is linked to uncertainties in dynamical changes, primarily in the polar vortex
- Large decadal variability in the Arctic vortex prevents an observational constraint on future Arctic recovery based on circulation
- Ozone-depleting substances and global warming drive ozone recovery spread equally; dynamical uncertainty affects primarily the latter

Supporting Information:

Supporting Information may be found in the online version of this article.

Correspondence to:

S. Benito-Barca,
s.benito@igeo.ucm-csic.es

Citation:

Benito-Barca, S., Abalos, M., Calvo, N., de la Cámara, A., Ayarzagüena, B., Chiodo, G., et al. (2026). On the role of dynamical uncertainties in the spread of Arctic ozone recovery projections. *Geophysical Research Letters*, *53*, e2025GL120212. https://doi.org/10.1029/2025GL120212

Received 28 OCT 2025
Accepted 23 APR 2026

Author Contributions:

Conceptualization: Samuel Benito-Barca, Marta Abalos, Natalia Calvo
Data curation: Samuel Benito-Barca
Formal analysis: Samuel Benito-Barca, Marta Abalos, Natalia Calvo, Alvaro de la Cámara, Blanca Ayarzagüena, Gabriel Chiodo
Methodology: Samuel Benito-Barca, Marta Abalos, Natalia Calvo
Resources: Hideharu Akiyoshi, Fraser Dennison, Patrick Jöckel, Béatrice Josse, Doug Kinnison, Olaf Morgenstern, David Plummer, Timofei Sukhodolov, Yousuke Yamashita, Shingo Watanabe
Software: Samuel Benito-Barca
Visualization: Samuel Benito-Barca

1. Introduction

Stratospheric ozone plays a vital role in the climate system. It protects the Earth's surface from harmful solar UV radiation, modulates the Earth's radiative budget and affects surface climate through coupling with the atmospheric circulation (Friedel et al., 2022; Ivy et al., 2017). Following the drastic reduction in the late 20th century due to the increase in anthropogenic ozone-depleting substances (ODS), the global ozone layer is expected to recover to pre-1980 levels over the 21st century thanks to the phasing-out of ODS concentrations in compliance

Writing – original draft: Samuel Benito-Barca
Writing – review & editing: Marta Abalos, Natalia Calvo, Alvaro de la Cámara, Blanca Ayarzagüena, Gabriel Chiodo

with the Montreal Protocol and its subsequent amendments (Chipperfield et al., 2017; Dhomse et al., 2018; Keeble et al., 2021). Particularly for the Arctic, stratospheric ozone is expected to reach 1980 values before mid-century and largely exceed those concentrations in the second half of the 21st century in mid- and high-level greenhouse gases (GHG) emission scenarios, the so-called "super-recovery" (WMO, 2022). However, there is large intermodel spread in the rates of Arctic ozone recovery, with return dates ranging from 2020 to 2050 for the RCP6.0 scenario (Table 3 of Dhomse et al. (2018)).

Apart from chemical sources and sinks, the distribution of ozone in the stratosphere is largely determined by the Brewer-Dobson circulation (BDC) and the stratospheric polar vortex (SPV). First, the BDC transports ozone from its source region to the pole in the winter hemisphere (Butchart, 2014). Second, the SPV acts as a strong transport barrier, preventing air exchange between middle and polar latitudes (Plumb, 2002; Waugh & Polvani, 2010). Consequently, a strong SPV prevents ozone mixing into polar latitudes and isolates cold polar air favoring the occurrence of very low temperatures and, therefore, the formation of polar stratospheric clouds, enhancing ozone depletion once sunlight returns in springtime (Dameris et al., 2021; Harris et al., 2010; Lawrence et al., 2020). Thus, Arctic ozone recovery over the 21st century is not only affected by the decline of ODS concentrations, but also by chemical and dynamical changes in the stratosphere driven by increasing GHG concentrations. The CO_2-induced radiative cooling of the stratosphere results in less ozone being destroyed in the upper stratosphere, increasing its concentration and making more ozone available for transport to the polar lower stratosphere (Fomichev et al., 2007; Match & Gerber, 2022). It is well-established from climate models that the BDC accelerates under increasing GHG concentrations (Butchart, 2014; Hardiman et al., 2014), thus enhancing ozone transport to the lower-middle polar stratosphere. However, trends in both the deep branch of the BDC residual circulation, the one reaching the Arctic stratosphere, and in its wave driving are very uncertain (Abalos et al., 2021). Even more uncertain is the response of the SPV to increasing GHG concentrations. Models differ widely in their projections of the mean strength of the SPV under climate change, with uncertainty even in the sign of the change (Ayarzagüena et al., 2020; Karpechko et al., 2022, 2024; Wu et al., 2019). A weaker SPV would imply a weaker barrier at high latitudes, which would facilitate ozone mixing across the vortex edge. The opposite would occur with a stronger SPV.

Overall, the large uncertainties in the response of the stratospheric dynamical features to climate change and the strong coupling between dynamical processes and stratospheric ozone suggest that the former may play an important role in the intermodel spread of the rate of Arctic ozone recovery. In this paper, we use output from models participating in the Chemistry-Climate Model Initiative, phases 1 (CCMI-1) and 2022 (CCMI-2022), to quantify the extent to which the intermodel spread in Arctic ozone recovery can be attributed to uncertainties in the projected evolution of the stratospheric circulation.

2. Data

We analyze simulations from 14 CCMI-1 models (Eyring et al., 2013; Morgenstern et al., 2017) and 9 models from CCMI-2022 (Plummer et al., 2021). For CCMI-1, we use REF-C2 simulations spanning from 1960 to 2100. These simulations use the A1 WMO-2010 scenario for ODS, observed surface concentrations of GHGs until 2005, and afterward they follow the RCP6.0 scenario for GHG. For CCMI-2022, we use REF-D2 simulations, which are analogous to the REF-C2 experiment but following the WMO-2018 baseline scenario for ODS concentrations and the SSP2-4.5 scenario for GHGs. Thus, the GHG forcing is slightly smaller and the ODS decline slightly slower in the CCMI-2022 than in the CCMI-1 simulations. Tables S1 and S2 in Supporting Information S1 list all the models, together with the ensemble size of each model and data availability. Note that the number of models with w* data is lower than with zonal wind data, which we have checked that does not significantly affect the results presented here.

For ozone observations, we use ozone concentrations from the Stratospheric Water and Ozone Satellite Homogenized (SWOOSH) database (Davis et al., 2016). SWOOSH merges vertically resolved ozone observations from different limb profiling satellite instruments. The version used (version 2.7) provides zonal-mean monthly mean ozone mixing ratios with a horizontal resolution of 2.5° latitude and 31 vertical levels, between 1 and 316 hPa, covering the period January 1984–December 2024. In addition, for zonal wind, we use monthly mean data from the ERA5 reanalysis (Hersbach et al., 2020).

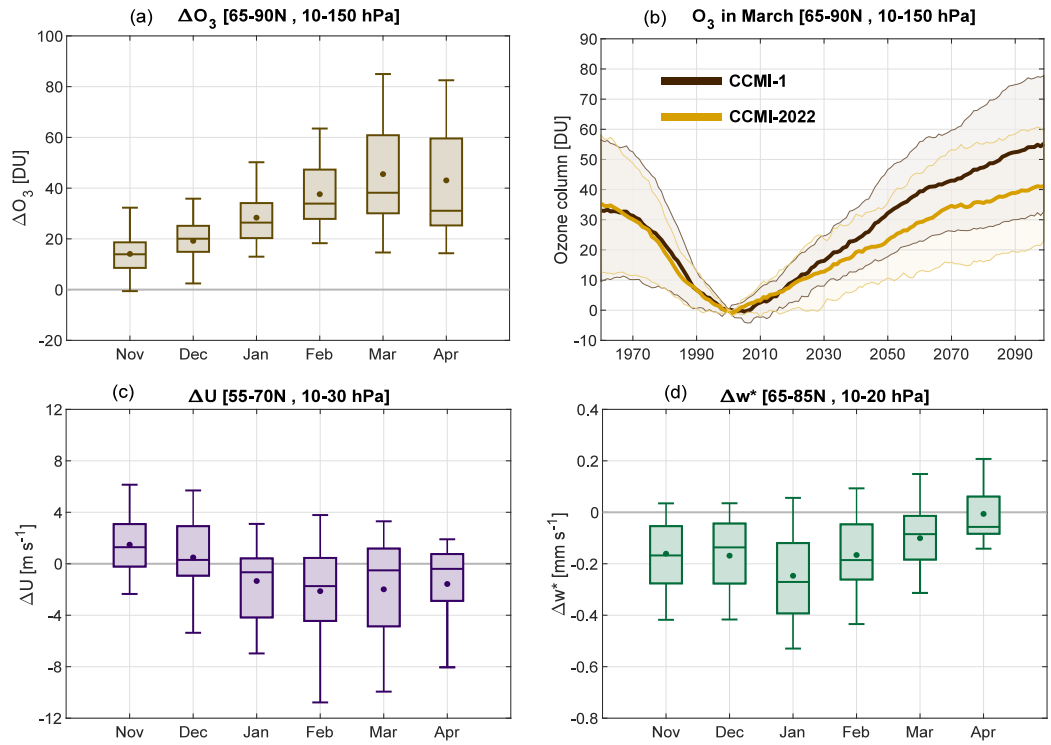

Figure 1. (a) Boxplots showing the monthly distribution of changes (2070–2099 minus 1991–2020) in CCMI-1 and CCMI-2022 simulations for Arctic lower-middle stratospheric ozone (65°N–90°N, 10–150 hPa). The size of the boxes represents the interquartile range of the data, while the whiskers extend from the 5th to 95th percentiles. The horizontal lines inside the boxes correspond to the median, while the dot shows the mean. (b) Twenty-one-year running mean time series of Arctic ozone in March from CCMI-1 (dark brown) and CCMI-2022 (light brown) multimodel mean normalized to the value in year 2000 in each simulation. The dark (light) brown envelope indicates the $\pm 1\sigma$ model uncertainty of the CCMI-1 (CCMI-2022) MMM. (c, d) Same as (a) but for (c) polar vortex strength (zonal wind averaged over 55°N–70°N, 10–30 hPa) and (d) polar downwelling (vertical component of the residual circulation averaged over 65°N–85°N, 10–20 hPa).

3. Results

3.1. Projected Changes and Spread Across Models

We first analyze ozone changes between the present period (1991–2020) and the end of the 21st century (2070–2099) for each individual month from November to April (Figure 1a). We define our region of interest as that in the lower-middle Arctic stratosphere (65°N–90°N, 10–150 hPa). All months show ozone recovery, although March is the month when ozone recovery and its inter-model spread (5th–95th percentile range) reach their maxima. This is because March is the month when Arctic ozone depletion is largest, and when the accumulation of ozone in the Arctic transported by the residual circulation is most noticeable (Brasseur & Solomon, 2005). Therefore, the remainder of this paper examines ozone recovery in March. Figure 1b shows the time evolution of March partial ozone column for the multimodel means (MMM), computed as the mean of the ensemble mean of all models, of CCMI-1 and CCMI-2022. Both the MMM and the uncertainty are similar in both data sets up to about 2030, and after 2030 the projected MMM ozone recovery in CCMI-1 is slightly larger than in CCMI-2022. However, despite the use of different external forcing scenarios and their potential influence on ozone recovery, the difference between CCMI-1 and CCMI-2022 MMMs is not significant due to the large intermodel spread. Importantly, the spread is of similar magnitude to the MMM value, for both model subsets, in the rate of ozone depletion (1970–2000) and the rate of ozone recovery (2000–2100). Therefore, in the remainder of this study, CCMI-1 and CCMI-2022 simulations are combined to increase the sample size and thereby enhance the robustness of the results. For both subsets of models, the return to 1980 values in the Arctic is projected near mid-century for the MMM, while by the end of the century a large fraction of the models predicts ozone values above those in 1960, consistent with WMO (2018) and WMO (2022).

Figure 1c shows the changes in the mean strength of the polar vortex from November to April. In this case, the use of CCMI-1 and CCMI-2022 together is justified because the net future response of the polar vortex does not depend on the climate scenario studied in the CCMs examined here (not shown), in agreement with previous studies (Karpechko et al., 2022). The uncertainty in the sign of the polar vortex change is present in all months, although February and March have the largest intermodel spread (Figure 1c). This large uncertainty and its seasonality is consistent with previous studies that have analyzed the response of the polar vortex to climate change (Karpechko et al., 2022; Manzini et al., 2014; Simpson et al., 2018). Arctic ozone abundances are not only largely controlled by the SPV, but also by polar downwelling. Thus, changes in the deep branch of the residual circulation can exert a sizable influence on ozone: these are shown in Figure 1d. Polar downwelling shows a robust increase in all months, with the largest MMM acceleration and intermodel spread occurring in January. However, in the remainder of the paper, we analyze changes in polar downwelling in February and March, because trends in these months are the most correlated with ozone recovery in March (not shown), and still display substantial spread across models. To summarize, Figure 1 shows that Arctic ozone recovery is a robust feature in CCMI models, but the recovery rates are highly uncertain. In addition, models show sizable uncertainty in the future evolution of key dynamical features that modulate polar ozone, that is, the SPV and the deep branch of the BDC residual circulation.

3.2. Role of the Stratospheric Dynamics Projections on the Spread in Arctic Ozone Recovery

Given the large uncertainty in the projected changes in ozone and stratospheric dynamics (SPV and residual circulation), it is pertinent to ask if they are related. That is, can the spread in Arctic ozone recovery be explained by the spread of the future evolution of the stratospheric circulation? The scatter-plots in Figure 2 show Arctic ozone changes versus the corresponding changes in the SPV and polar downwelling for each individual simulation. A strong negative correlation ($r = -0.77$) is found between changes in Arctic ozone recovery and the polar vortex (Figure 2a). This means that around 60% (r^2) of the inter-simulation variance in the Arctic ozone recovery is linearly explained by uncertainties in the future evolution of the polar vortex. The simulations with the most pronounced weakening of the polar vortex also project the largest Arctic ozone recovery by the end of the century, and vice versa.

The correlation coefficient between changes in Arctic ozone recovery and polar downwelling is slightly lower ($r = -0.58$, Figure 2b). Thus, one third of the variance in Arctic ozone recovery can be attributed to uncertainty in the projected enhancement of polar downwelling. The negative correlation coefficient indicates that the stronger the acceleration in polar downwelling, the faster the ozone recovery. This is consistent with enhanced ozone advection from the tropical stratosphere to the Arctic polar cap. Note that the variance explained by uncertainties in w* projections is not independent of that explained by uncertainties in SPV projections, as the SPV and residual circulation are coupled through the TEM momentum balance and their changes are not entirely independent (Figure S1 in Supporting Information S1). If both ΔU and Δw^* are used together as predictors in a multiple linear regression (MLR) model, the explained ozone recovery variance is 75% (not shown).

Our results are robust to the methodological details: they are very similar when the correlation coefficients are calculated considering CCMI-1 and CCMI-2022 separately (Table S3 in Supporting Information S1). Therefore, the relationship between future changes in ozone and dynamical features does not depend on the emissions scenario used here, nor on the generation of CCMs. The correlation coefficients are also very similar using ensemble means ($r = -0.67$ for SPV and $r = -0.52$ for w*). Note that, if the correlation between ozone and SPV changes is calculated only with the simulations with available w* data, the correlation is slightly higher (-0.81), which confirms the higher variance explained by the SPV compared to downwelling is not an artifact of the different data availability. Lastly, removing outliers such as the NIWA model, only decreases the correlation slightly ($r = -0.68$ for SPV).

Next, we look at the time evolution of Arctic ozone by grouping the simulations according to their change in the SPV and polar downwelling. Note that the simulations in each group when we separate according to the SPV are not necessarily the same as when we separate according to the polar downwelling (Figure S1 in Supporting Information S1). For the polar vortex, Figure 2c shows the one-third of simulations with the largest future vortex weakening in blue and the one-third of simulations that project a strengthening of the vortex in red. We find that the ozone evolution, both in the past and in the future, is significantly different between the two subsets of simulations at the 95% confidence level, with the simulations displaying the largest vortex weakening simulating

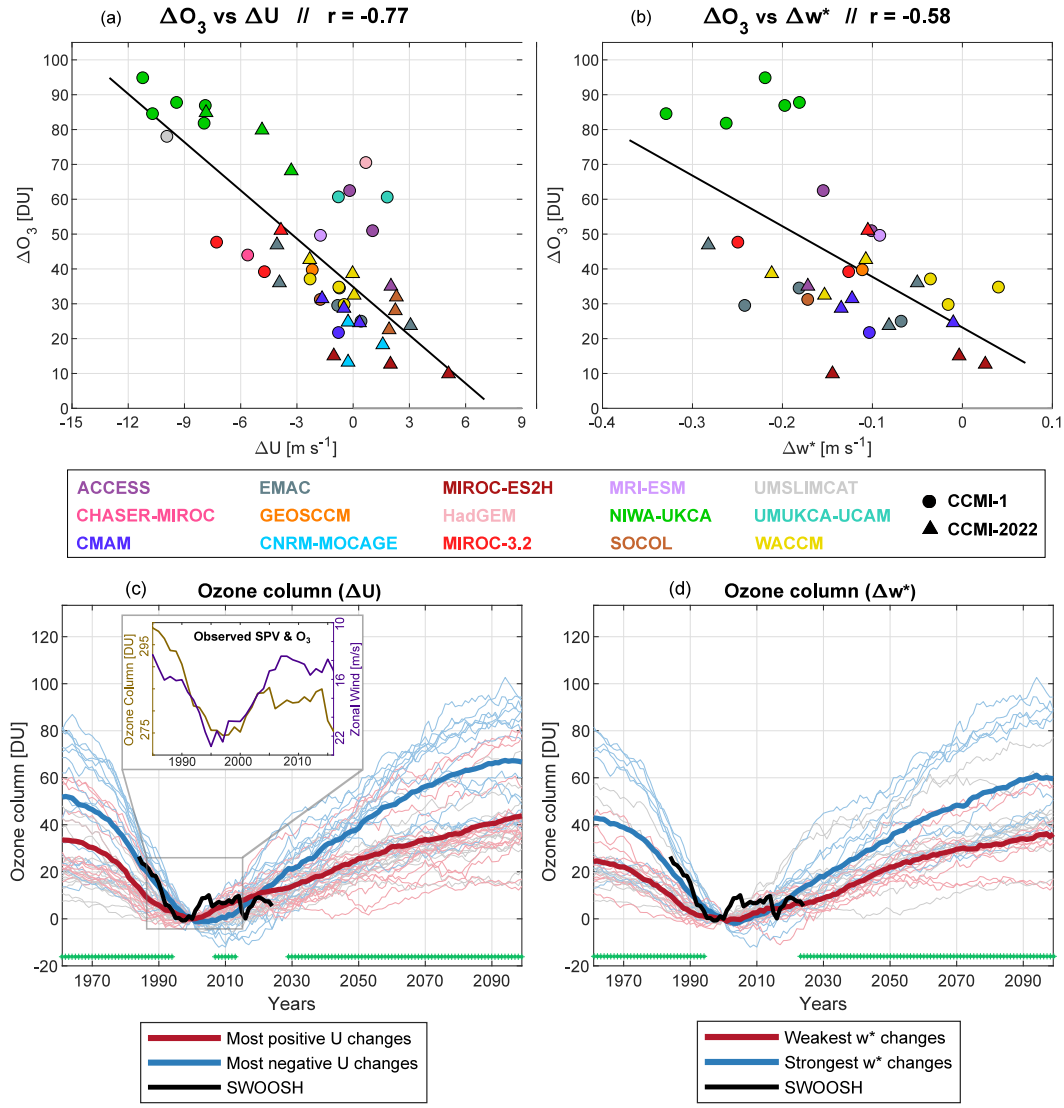

Figure 2. (a, b) Scatter-plot of changes (2070–2099 minus 1991–2020) in Arctic ozone versus (a) polar vortex and (b) polar downwelling. Each point corresponds to an individual simulation. Circles (triangles) depict CCMI-1 (CCMI-2022) models and colors indicate the model. Numbers in the title indicate the Pearson's correlation coefficient across simulations. The thick black line represents the linear least squares fit. (c, d) Time series of March Arctic ozone (65°N–90°N, 10–150 hPa) normalized to the year 2000 value for each simulation. In panel (c), the blue lines represent the third of simulations with the most negative changes in the polar vortex in panel (a), while the red lines represent the third with positive change. The embedded figure shows Stratospheric Water and Ozone Satellite Homogenized (SWOOSH) observations of Arctic ozone in light brown and the ERA5 polar vortex strength (February–March) in purple. In panel (d), blue (red) lines depict the third of simulations with the strongest (weakest) acceleration of polar downwelling in panel (b). Thick lines represent the mean of each group. The gray lines represent the remainder of the simulations (central tercile). The black line represents the SWOOSH observations. Green dots indicate when the two groups of simulations (blue and red) are significantly different at 95% using a *t*-test. All series have applied an 11-year running mean.

the strongest ozone recovery rate. Regarding polar downwelling (Figure 2d), the group of simulations with the strongest enhancement in downwelling (blue curves) shows faster ozone recovery than the simulations with the weakest acceleration in downwelling (red curves).

Figures 2c and 2d also reveal that simulations which project the largest change in ozone (and in the SPV and/or w*) in the future also simulate the largest ozone loss in the past. Compared to observations (black line), these simulations (blue lines) seem to be the ones that best match the observed ozone loss rate, potentially helping to better constrain future ozone recovery. However, these same simulations have unrealistically strong SPV

climatologies in the present period (Figure S2 in Supporting Information S1), which limits our confidence in their projections. We suggest that the apparent agreement in the past ozone evolution (1985–2000) between observations and this group of models arises mainly from the large dynamical variability on interannual to decadal timescales, and in particular from the strong vortex observed in the 90s (small panel in Figure 2c). As expected, the free-running simulations are not able to capture the timing of this unforced variability. This is confirmed by the disagreement in the period 2000–2010: the observed ozone increase, related to the weaker vortex in the 2000s, is not captured by any of the simulations, that instead show lower values. Thus, we conclude that an emergent constraint on the Arctic ozone recovery cannot be established based on circulation.

3.3. Contribution of ODS and GW to the Spread in Arctic Ozone Recovery Rates

The previous section analyzed how the intermodel spread of the projected evolution of the stratospheric circulation affects the spread in ozone recovery rates. Next, we address how external forcings, namely GHGs and ODS, affect ozone recovery and its spread. To do so, we performed a MLR analysis of the evolution of Arctic ozone including GHG-driven global warming (GW) and ODS as regressors (Mindlin et al., 2021):

$$O_3(t) = \alpha \cdot \mathrm{GW}(t) + \beta \cdot \mathrm{ODS}(t) + \epsilon(t) \quad (1)$$

In Equation 1, all variables represent the change in March with respect to the year 2000. O_3 refers to the Arctic partial column ozone, the GW index is computed as the area-weighted global mean air temperature at 1,000 hPa, and the ODS index is calculated using the equivalent effective stratospheric chlorine (EESC), as by Newman et al. (2007), averaged within the polar cap (65N°–90°N) at 50 hPa. The residual is denoted by $\epsilon(t)$. We apply the MLR to each individual simulation and construct the time series of ozone associated with each forcing. Then, the MMM of these time series and their standard deviations are calculated using all the ensemble members. Since CCMI-1 and CCMI-2022 follow different emission scenarios, their relative ODS and GHG contributions to ozone recovery could differ; thus, Figures 3a–3d show the results for each set of simulations separately. We note that the results do not change if we consider CO_2 surface concentrations as a regressor instead of the GW index (not shown).

The Arctic ozone evolution and the intermodel spread are well reconstructed by the MLR both in the past and in the future. The regression models in Figures 3a and 3b are able to simulate the loss in springtime stratospheric ozone at the end of the 20th century and the subsequent recovery throughout the 21st century, exceeding pre-1980 values at the end of the century, consistent with Figure 1a. Both CCMI-1 (Figure 3c) and CCMI-2022 (Figure 3d) results show that ozone depletion before the year 2000 (rate and spread across simulations) is entirely explained by the increase in EESC, with a negligible opposite-sign contribution from the increase in GHGs. In the 21st century, the decrease in EESC also dominates the behavior of ozone. However, the ozone recovery, and particularly the super-recovery at the end of the century, cannot be explained without the contribution of GW. These results are highly consistent with those by Dhomse et al. (2018), who used a different methodology based on the CCMI-1 sensitivity simulations, in which either ODS or GHG concentrations were fixed to 1960 levels. Indeed, for the models providing these sensitivity simulations, we obtain results which are consistent with our MLR estimates (not shown).

Even though both CCMI-1 and CCMI-2022 sets of models project a positive contribution of both forcings to ozone recovery, the rate of recovery due to each of the forcings and the ratio of the contributions do differ. In CCMI-1, the mean contribution to ozone recovery from ODS reduction and GHG increase is similar. In CCMI-2022 the GW contribution is lower, consistent with a more moderate emissions scenario (SSP2-4.5 vs. RCP6.0), which explains the slight difference between CCMI-1 and CCMI-2022 in Figure 1b. Interestingly, both ODS and GHGs contribute significantly to the spread in ozone recovery rates in both CCMI-1 and CCMI-2022.

Finally, we analyze how changes in circulation affect the ODS and GW contributions to ozone recovery. For this purpose, Figures 3e–3h show the ozone time series associated with each forcing, as in Figures 3c and 3d, but grouping the simulations according to the changes in the SPV (Figures 3e and 3g) and polar downwelling (Figures 3f and 3g). The GW contribution to ozone recovery (Figures 3e and 3f) is significantly different between simulations with extreme changes in both SPV and downwelling. The correlation across-simulations between ozone recovery associated with GW and future changes in SPV is −0.63, while the correlation with changes in polar downwelling is −0.52. This means that the simulations with the largest weakening of the SPV and/or the

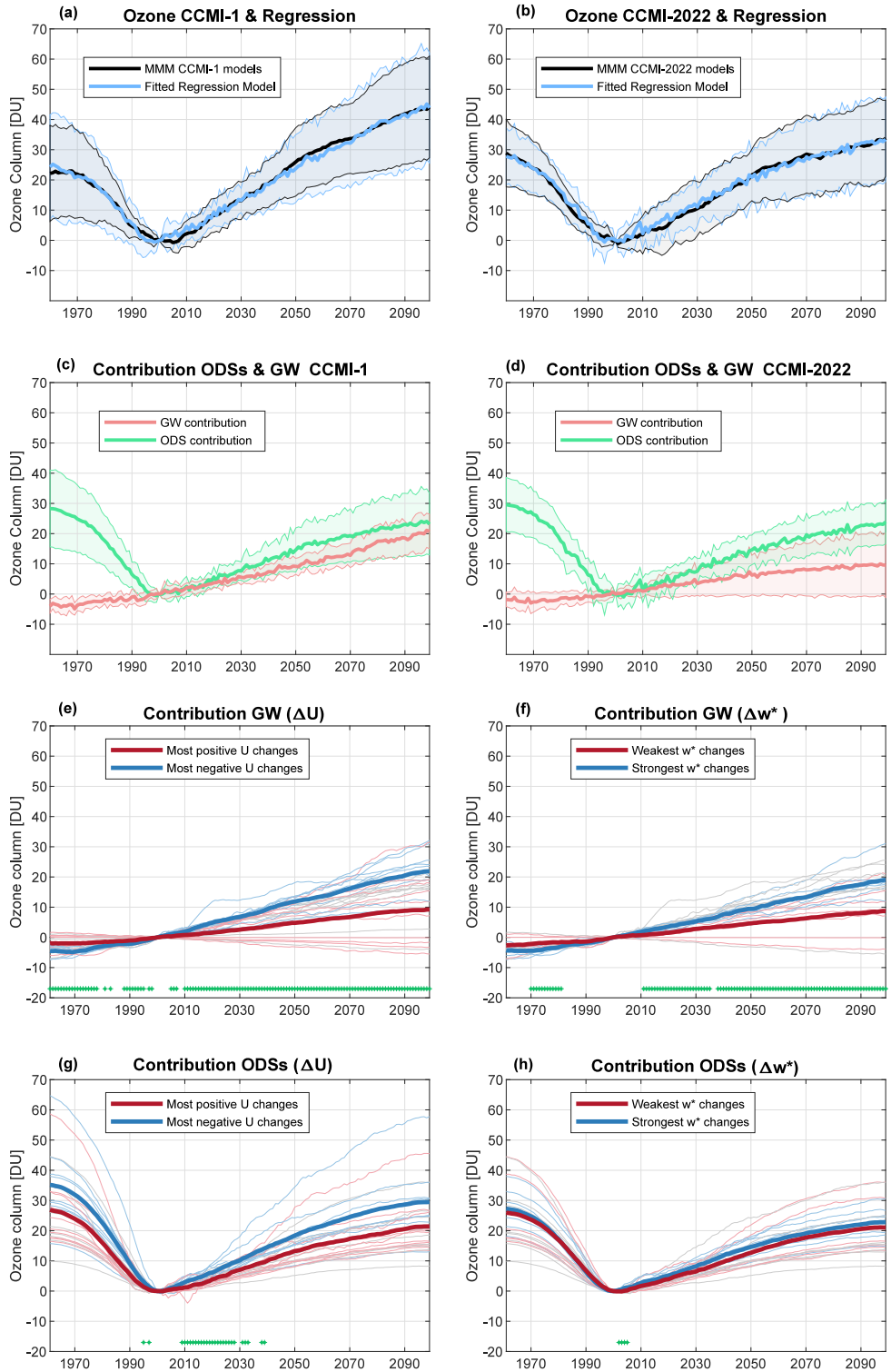

Figure 3. (a, b) Black line represents the MMM original time series of March Arctic ozone (65°N–90°N, 10–150 hPa) normalized to year 2000, with a 21-year running mean applied, while the blue line displays the total linear fit from the regression model for a sub-set of (a) CCMI-1 and (b) CCMI-2022 simulations. (c, d) Contributions of ozone-depleting substances (ODS) (green line) and global warming (GW) (red line) to the Arctic ozone evolution for (c) CCMI-1 and (d) CCMI-2022 simulations. In panels (a–d), light envelopes indicate the multimodel standard deviation. (e–h) Same as (a, b) but for (e, f) GW contribution and (g, h) ODS contribution.

strongest acceleration of polar downwelling simulate a faster ozone recovery associated with GW. In contrast, the ODS contribution to ozone recovery (Figures 3g and 3h) presents non-significant differences between the "blue" and "red" subsets of simulations at the end of the century (despite similar differences to the GW contribution between subsets in Figure 3g, the larger spread here makes them non-significant). This means that the contribution of ODS decline to ozone recovery does not occur significantly through changes in dynamical characteristics. In contrast, uncertainties in the dynamical changes affecting Arctic ozone super-recovery are related to uncertainties in the GW contribution. These results suggest that the SPV influences Arctic ozone recovery mainly through modulation of the lateral mixing of ozone into the polar region, rather than by influencing the heterogeneous chemistry. However, further mechanistic analyses beyond the scope of the study are needed to disentangle these effects.

4. Summary and Discussion

This study quantifies the role of uncertainties in the future evolution of the Arctic polar vortex and BDC residual circulation in the spread in Arctic ozone recovery projections using simulations from the Chemistry-Climate Model Initiative, phases 1 and 2022. The main findings of our study are summarized here:

- Seventy-five percent of the intermodel spread in the Arctic ozone recovery in March can be attributed to uncertainties in dynamical trends in late winter. Sixty percent is related to uncertainties in SPV trends, and 33% to uncertainties in polar downwelling trends. The larger the weakening of the SPV and/or the strengthening of polar downwelling, the faster the recovery of Arctic ozone.
- The simulated ozone recovery can be clearly separated into distinct groups based on dynamical changes. However, the large decadal variability of the Arctic stratosphere, in particular of the SPV during the 1990s and 2000s, prevents the identification of an observational constraint on future ozone recovery.
- The contributions of ODS and GHG-driven GW are both important to explain the uncertainty in ozone recovery rates. GW affects ozone recovery spread through uncertainties in stratospheric circulation trends, while the contribution of ODS to ozone recovery through changes in dynamical characteristics is negligible.

A suggestive result is that the spread in ozone recovery is better explained by uncertainties in the SPV than in polar downwelling. However, this does not necessarily imply that the increase in Arctic ozone is more closely linked to changes in the polar vortex than to the acceleration of polar downwelling, and thus to enhanced ozone advection. A plausible explanation is related to ozone-climate feedbacks. On the one hand, the high correlation between Arctic ozone and the SPV could be amplified by positive feedbacks. Larger weakening of the SPV implies a weaker transport barrier and therefore a faster Arctic ozone recovery. In turn, larger Arctic ozone concentrations lead to larger radiative heating in the polar stratosphere during late winter and spring, thus reducing the meridional temperature gradient and weakening even more the SPV due to the thermal wind balance. This positive feedback is consistent with the results of Chiodo et al. (2023), who explicitly calculated the impact of ozone recovery on the polar vortex in early spring in two CCMs, showing a larger vortex weakening in the model with larger Arctic ozone recovery. On the other hand, the link between ozone recovery and polar downwelling could be affected by negative feedbacks. The GHG-driven acceleration of the residual circulation implies higher ozone advection to the Arctic. In contrast, as has been extensively documented in the case of the Antarctic ozone hole (Abalos et al., 2019; McLandress et al., 2010; Polvani et al., 2018, 2019) and recently shown by Chiodo et al. (2023) for the future in the Arctic, increasing ozone concentrations leads to a reduction in polar cap downwelling, and therefore less transport of ozone into the polar vortex. This is due to the warming of the polar stratosphere and associated weakening of the vortex in late winter, which advances the final vortex breakup and leads to reduced wave propagation and dissipation, and thus weaken the residual circulation. This is also consistent with other recent studies (e.g., Hufnagl et al., 2023), showing a dampening of the BDC acceleration under increasing CO_2 due to ozone feedbacks. Thus, while ozone feedbacks may enhance the connection between Arctic ozone recovery and the SPV, they may obscure the coupling between Arctic ozone accumulation and polar downwelling.

Another emerging factor that could weaken the link between Arctic ozone recovery and residual circulation trends could be the tropical tropopause expansion. Match and Gerber (2025) argued that tropical tropospheric expansion reduces ozone in the tropical lowermost stratosphere, and these reductions could then be transported laterally into the extratropical lower stratosphere. This could be contributing to weakening the correlation between Arctic ozone recovery and polar downwelling, since tropospheric expansion and strengthened downwelling driven by

rising GHG concentrations have opposite effects on Arctic lower stratospheric ozone. However, we checked that the Arctic ozone recovery rates are not significantly correlated with the tropical tropopause pressure across model simulations (not shown).

In short, our results clarify how the spread in future changes of the NH polar vortex and the deep branch of the residual circulation contribute to the spread in Arctic ozone recovery. They highlight the critical need to reduce uncertainties in the stratospheric circulation response to GHGs, especially in polar vortex trends, to better constrain projections of Arctic ozone recovery over the 21st century.

Conflict of Interest

The authors declare no conflicts of interest relevant to this study.

Availability Statement

The CCMI-1 and CCMI-2022 data used in this study are stored at the Centre for Environmental Data Analysis (CEDA) and have been obtained through the British Atmospheric Data Centre (BADC) archive. CCMI-1 data have been downloaded from https://data.ceda.ac.uk/badc/wcrp-ccmi/data/CCMI-1/output and CCMI-2022 from https://data.ceda.ac.uk/badc/ccmi/data/post-cmip6/ccmi-2022. The SWOOSH data set is available at https://www.esrl.noaa.gov/csd/groups/csd8/swoosh/ (last access: February 2025). Data from the ERA-5 reanalysis (Hersbach et al., 2020) are available in the Climate Data Store at Hersbach et al. (2023).

Acknowledgments
MA, BA, and NC acknowledge funding from the Spanish National projects reference PID2021-124772OB-I00 and PID2024-158151NB-I00. SBB was supported by the Spanish National Research Council: Grant 20233AT034. AC is supported by the Spanish Research Agency: Grant PID2022-136316NB-I00. GC acknowledges funding from the European Commission via the ERC StG Grant 101078127. SW acknowledges the Earth Simulator at JAMSTEC and funding from the MEXT-SENTAN program (Grant JPMXD0722681344). HA acknowledges the NIES supercomputer (NEC SX-Aurora TSUBASA) and funding from KAKENHI (JP24K00700) of Japan. PJ acknowledges support from DKRZ and BMBF for HPC and data archiving resources used in EMAC simulations within the ESCiMo project. TS acknowledges funding from the SNSF (project STOA, Grant 200021L-228149) and the use of ETH cluster EULER and the CSCS (projects s1191 and s1144) to perform SOCOL simulations. We also acknowledge the support of the CEDA in hosting the publicly available archive of CCMI model outputs.

References

Abalos, M., Calvo, N., Benito-Barca, S., Garny, H., Hardiman, S. C., Lin, P., et al. (2021). The Brewer-Dobson circulation in CMIP6. *Atmospheric Chemistry and Physics*, *21*(17), 13571–13591. https://doi.org/10.5194/acp-21-13571-2021

Abalos, M., Polvani, L., Calvo, N., Kinnison, D., Ploeger, F., Randel, W., & Solomon, S. (2019). New insights on the impact of ozone-depleting substances on the Brewer-Dobson circulation. *Journal of Geophysical Research: Atmospheres*, *124*(5), 2435–2451. https://doi.org/10.1029/2018JD029301

Ayarzagüena, B., Charlton-Perez, A. J., Butler, A. H., Hitchcock, P., Simpson, I. R., Polvani, L. M., et al. (2020). Uncertainty in the response of sudden stratospheric warmings and stratosphere-troposphere coupling to quadrupled CO_2 concentrations in CMIP6 models. *Journal of Geophysical Research: Atmospheres*, *125*(6), 1–21. https://doi.org/10.1029/2019JD032345

Brasseur, G. P., & Solomon, S. (2005). *Aeronomy of the middle atmosphere: Chemistry and physics of the stratosphere and mesosphere* (3rd ed.). Springer. https://doi.org/10.1007/1-4020-3824-0

Butchart, N. (2014). The Brewer-Dobson circulation. *Reviews of Geophysics*, *52*(2), 157–184. https://doi.org/10.1002/2013RG000448

Chiodo, G., Friedel, M., Seeber, S., Domeisen, D., Stenke, A., Sukhodolov, T., & Zilker, F. (2023). The influence of future changes in springtime Arctic ozone on stratospheric and surface climate. *Atmospheric Chemistry and Physics*, *23*(18), 10451–10472. https://doi.org/10.5194/acp-23-10451-2023

Chipperfield, M. P., Bekki, S., Dhomse, S., Harris, N. R. P., Hassler, B., Hossaini, R., et al. (2017). Detecting recovery of the stratospheric ozone layer. *Nature*, *549*(7671), 211–218. https://doi.org/10.1038/nature23681

Dameris, M. G., Loyola, D., Nützel, M., Coldewey-Egbers, M., Lerot, C., Romahn, F., & Van Roozendael, M. (2021). Record low ozone values over the Arctic in boreal spring 2020. *Atmospheric Chemistry and Physics*, *21*(2), 617–633. https://doi.org/10.5194/acp-21-617-2021

Davis, S. M., Rosenlof, K. H., Hassler, B., Hurst, D. F., Read, W. G., Vömel, H., et al. (2016). The stratospheric water and ozone satellite homogenized (SWOOSH) database: A long-term database for climate studies. *Earth System Science Data*, *8*(2), 461–490. https://doi.org/10.5194/essd-8-461-2016

Dhomse, S. S., Kinnison, D., Chipperfield, M. P., Salawitch, R. J., Cionni, I., Hegglin, M. I., et al. (2018). Estimates of ozone return dates from chemistry-climate model initiative simulations. *Atmospheric Chemistry and Physics*, *18*(11), 8409–8438. https://doi.org/10.5194/acp-18-8409-2018

Eyring, V., Lamarque, J.-F., Hess, P., Arfeuille, F., Bowman, K., Chipperfiel, M. P., et al. (2013). Overview of IGAC/SPARC chemistry-climate model initiative (CCMI) community simulations in support of upcoming ozone and climate assessments. *SPARC Newsletter*, *40*, 48–66.

Fomichev, V. I., Jonsson, A. I., de Grandpré, J., Beagley, S. R., McLandress, C., Semeniuk, K., & Shepherd, T. G. (2007). Response of the middle atmosphere to CO_2 doubling: Results from the Canadian middle atmosphere model. *Journal of Climate*, *20*(7), 1121–1144. https://doi.org/10.1175/JCLI4030.1

Friedel, M., Chiodo, G., Stenke, A., Domeisen, D. I. V., & Peter, T. (2022). Effects of Arctic ozone on the stratospheric spring onset and its surface impact. *Atmospheric Chemistry and Physics*, *22*(21), 13997–14017. https://doi.org/10.5194/acp-22-13997-2022

Hardiman, S. C., Butchart, N., & Calvo, N. (2014). The morphology of the Brewer-Dobson circulation and its response to climate change in CMIP5 simulations. *Quarterly Journal of the Royal Meteorological Society*, *140*(683), 1958–1965. https://doi.org/10.1002/qj.2258

Harris, N. R. P., Lehmann, R., Rex, M., & Von Der Gathen, P. (2010). A closer look at Arctic ozone loss and polar stratospheric clouds. *Atmospheric Chemistry and Physics*, *10*(17), 8499–8510. https://doi.org/10.5194/acp-10-8499-2010

Hersbach, H., Bell, B., Berrisford, P., Biavati, G., Horányi, A., Muñoz Sabater, J., et al. (2023). ERA5 hourly data on pressure levels from 1940 to present [Dataset]. *Copernicus Climate Change Service (C3S) Climate Data Store (CDS)*. https://doi.org/10.24381/cds.bd0915c6

Hersbach, H., Bell, B., Berrisford, P., Hirahara, S., Horányi, A., Muñoz-Sabater, J., et al. (2020). The ERA5 global reanalysis. *Quarterly Journal of the Royal Meteorological Society*, *146*(730), 1999–2049. https://doi.org/10.1002/qj.3803

Hufnagl, L., Eichinger, R., Garny, H., Birner, T., Kuchař, A., Jöckel, P., & Graf, P. (2023). Stratospheric ozone changes damp the CO_2-Induced acceleration of the Brewer–Dobson circulation. *Journal of Climate*, *36*(10), 3305–3320. https://doi.org/10.1175/JCLI-D-22-0512.1

Ivy, D. J., Solomon, S., Calvo, N., & Thompson, D. W. J. (2017). Observed connections of Arctic stratospheric ozone extremes to northern hemisphere surface climate. *Environmental Research Letters*, *12*(2), 024004. https://doi.org/10.1088/1748-9326/aa57a4

Karpechko, A. Y., Afargan-Gerstman, H., Butler, A. H., Domeisen, D. I. V., Kretschmer, M., Lawrence, Z., et al. (2022). Northern hemisphere stratosphere-troposphere circulation change in CMIP6 models: 1. Inter-model spread and scenario sensitivity. *Journal of Geophysical Research: Atmospheres*, *127*(18), e2022JD036992. https://doi.org/10.1029/2022JD036992

Karpechko, A. Y., Wu, Z., Simpson, I. R., Kretschmer, M., Afargan-Gerstman, H., Butler, A. H., et al. (2024). Northern hemisphere stratosphere-troposphere circulation change in CMIP6 models: 2. Mechanisms and sources of the spread. *Journal of Geophysical Research: Atmospheres*, *129*(13), 1–23. https://doi.org/10.1029/2024JD040823

Keeble, J., Hassler, B., Banerjee, A., Checa-Garcia, R., Chiodo, G., Davis, S., et al. (2021). Evaluating stratospheric ozone and water vapour changes in CMIP6 models from 1850 to 2100. *Atmospheric Chemistry and Physics*, *21*(6), 5015–5061. https://doi.org/10.5194/acp-21-5015-2021

Lawrence, Z. D., Perlwitz, J., Butler, A. H., Manney, G. L., Newman, P. A., Lee, S. H., & Nash, E. R. (2020). The remarkably strong Arctic stratospheric polar vortex of winter 2020: Links to record-breaking Arctic oscillation and ozone loss. *Journal of Geophysical Research: Atmospheres*, *125*(22), 1–21. https://doi.org/10.1029/2020JD033271

Manzini, E., Karpechko, A. Y., Anstey, J., Baldwin, M. P., Black, R. X., Cagnazzo, C., et al. (2014). Northern winter climate change: Assessment of uncertainty in CMIP5 projections related to stratosphere-troposphere coupling. *Journal of Geophysical Research: Atmospheres*, *119*(13), 7979–7998. https://doi.org/10.1002/2013JD021403

Match, A., & Gerber, E. P. (2022). Tropospheric expansion under global warming reduces tropical lower stratospheric ozone. *Geophysical Research Letters*, *49*(19), e2022GL099463. https://doi.org/10.1029/2022GL099463

Match, A., & Gerber, E. P. (2025). The double dip: How tropospheric expansion counteracts increases in extratropical stratospheric ozone under global warming. *Geophysical Research Letters*, *52*(9), e2024GL112409. https://doi.org/10.1029/2024GL112409

McLandress, C., Jonsson, A. I., Plummer, D. A., Reader, M. C., Scinocca, J. F., & Shepherd, T. G. (2010). Separating the dynamical effects of climate change and ozone depletion. Part I: Southern hemisphere stratosphere. *Journal of Climate*, *23*(18), 5002–5020. https://doi.org/10.1175/2010JCLI3586.1

Mindlin, J., Shepherd, T. G., Vera, C., & Osman, M. (2021). Combined effects of global warming and ozone depletion/recovery on southern hemisphere atmospheric circulation and regional precipitation. *Geophysical Research Letters*, *48*(12), 1–9. https://doi.org/10.1029/2021GL092568

Morgenstern, O., Hegglin, M., Rozanov, E., O'Connor, F., Luke Abraham, N., Akiyoshi, H., et al. (2017). Review of the global models used within phase 1 of the chemistry-climate model initiative (CCMI). *Geoscientific Model Development*, *10*(2), 639–671. https://doi.org/10.5194/gmd-10-639-2017

Newman, P. A., Daniel, J. S., Waugh, D. W., & Nash, E. R. (2007). A new formulation of equivalent effective stratospheric chlorine (EESC). *Atmospheric Chemistry and Physics*, *7*(17), 4537–4552. https://doi.org/10.5194/acp-7-4537-2007

Plumb, R. A. (2002). Large-scale stratospheric transport processes. *Journal of the Meteorological Society of Japan. Series II*, *80*(4B), 793–809. https://doi.org/10.2151/jmsj.80.793

Plummer, D., Nagashima, T., Tilmes, S., Archibald, A., Chiodo, G., Fadnavis, S., et al. (2021). CCMI-2022: A new set of chemistry-climate model initiative (CCMI) community simulations to update the assessment of models and support upcoming Ozone assessment activities. *SPARC Newsletter*, *57*, 22–30.

Polvani, L. M., Abalos, M., Garcia, R., Kinnison, D., & Randel, W. J. (2018). Significant weakening of Brewer-Dobson circulation trends over the 21st century as a consequence of the Montreal protocol. *Geophysical Research Letters*, *45*(1), 401–409. https://doi.org/10.1002/2017GL075345

Polvani, L. M., Wang, L., Abalos, M., Butchart, N., Chipperfield, M. P., Dameris, M., et al. (2019). Large impacts, past and future, of ozone-depleting substances on Brewer-Dobson circulation trends: A multimodel assessment. *Journal of Geophysical Research: Atmospheres*, *124*(13), 6669–6680. https://doi.org/10.1029/2018JD029516

Simpson, I. R., Hitchcock, P., Seager, R., Wu, Y., & Callaghan, P. (2018). The downward influence of uncertainty in the northern hemisphere stratospheric polar vortex response to climate change. *Journal of Climate*, *31*(16), 6371–6391. https://doi.org/10.1175/JCLI-D-18-0041.1

Waugh, D. W., & Polvani, L. M. (2010). The stratosphere: Dynamics, transport, and chemistry - Stratospheric polar vortices. *Geophysical Monograph Series*, *190*, 43–58.

WMO. (2018). *Scientific assessment of Ozone depletion: Global ozone research and monitoring project -- report no. 58*. World Meteorological Organization.

WMO. (2022). *Scientific assessment of ozone depletion: Global ozone research and monitoring project -- GAW report no. 278*. World Meteorological Organization.

Wu, Y., Simpson, I. R., & Seager, R. (2019). Intermodel spread in the northern hemisphere stratospheric polar vortex response to climate change in the CMIP5 models. *Geophysical Research Letters*, *46*(22), 13290–13298. https://doi.org/10.1029/2019GL085545

References From the Supporting Information

Akiyoshi, H., Kadowaki, M., Yamashita, Y., & Nagatomo, T. (2023). Dependence of column ozone on future ODSs and GHGs in the variability of 500-ensemble members. *Scientific Reports*, *13*(1), 1–12. https://doi.org/10.1038/s41598-023-27635-y

Akiyoshi, H., Nakamura, T., Miyasaka, T., Shiotani, M., & Suzuki, M. (2016). A nudged chemistry-climate model simulation of chemical constituent distribution at northern high-latitude stratosphere observed by SMILES and MLS during the 2009/2010 stratospheric sudden warming. *Journal of Geophysical Research: Atmospheres*, *121*(3), 1361–1380. https://doi.org/10.1002/2015JD023334

Bednarz, E. M., Maycock, A. C., Abraham, N. L., Braesicke, P., Dessens, O., & Pyle, J. A. (2016). Future Arctic ozone recovery: The importance of chemistry and dynamics. *Atmospheric Chemistry and Physics*, *16*(18), 12159–12176. https://doi.org/10.5194/acp-16-12159-2016

Cussac, M., Marécal, V., Thouret, V., Josse, B., & Sauvage, B. (2020). The impact of biomass burning on upper tropospheric carbon monoxide: A study using MOCAGE global model and IAGOS airborne data. *Atmospheric Chemistry and Physics*, *20*(15), 9393–9417. https://doi.org/10.5194/acp-20-9393-2020

Dennison, F., & Woodhouse, M. T. (2023). ACCESS-CM2-Chem: Evaluation of southern hemisphere ozone and its effect on the southern annular mode. *Journal of Southern Hemisphere Earth Systems Science*, *73*(1), 17–29. https://doi.org/10.1071/es22015

Deushi, M., & Shibata, K. (2011). Development of a meteorological research institute chemistry-climate model version 2 for the study of tropospheric and stratospheric chemistry. *Papers in Meteorology and Geophysics*, *62*, 1–46. https://doi.org/10.2467/mripapers.62.1

Garcia, R. R., Smith, A. K., Kinnison, D. E., de la Cámara, Á., & Murphy, D. J. (2017). Modification of the gravity wave parameterization in the whole atmosphere community climate model: Motivation and results. *Journal of the Atmospheric Sciences*, *74*(1), 275–291. https://doi.org/10.1175/JAS-D-16-0104.1

Gettelman, A., Mills, M. J., Kinnison, D. E., Garcia, R. R., Smith, A. K., Marsh, D. R., et al. (2019). The whole atmosphere community climate model version 6 (WACCM6). *Journal of Geophysical Research: Atmospheres*, *124*(23), 12380–12403. https://doi.org/10.1029/2019JD030943

Hardiman, S. C., Butchart, N., O'Connor, F. M., & Rumbold, S. T. (2017). The Met Office HadGEM3-ES chemistry-climate model: Evaluation of stratospheric dynamics and its impact on ozone. *Geoscientific Model Development*, *10*(3), 1209–1232. https://doi.org/10.5194/gmd-10-1209-2017

Imai, K., Manago, N., Mitsuda, C., Naito, Y., Nishimoto, E., Sakazaki, T., et al. (2013). Validation of ozone data from the superconducting submillimeter-wave limb-emission sounder (SMILES). *Journal of Geophysical Research: Atmospheres*, *118*(11), 5750–5769. https://doi.org/10.1002/jgrd.50434

Jöckel, P., Kerkweg, A., Pozzer, A., Sander, R., Tost, H., Riede, H., et al. (2010). Development cycle 2 of the modular Earth submodel system (MESSy2). *Geoscientific Model Development*, *3*(2), 717–752. https://doi.org/10.5194/gmd-3-717-2010

Jöckel, P., Tost, H., Pozzer, A., Kunze, M., Kirner, O., Brenninkmeijer, C. A. M., et al. (2016). Earth system chemistry integrated modelling (ESCiMo) with the modular Earth submodel system (MESSy) version 2.51. *Geoscientific Model Development*, *9*(3), 1153–1200. https://doi.org/10.5194/gmd-9-1153-2016

Jonsson, A. I., de Grandpré, J., Fomichev, V. I., McConnell, J. C., & Beagley, S. R. (2004). Doubled CO_2-induced cooling in the middle atmosphere: Photochemical analysis of the ozone radiative feedback. *Journal of Geophysical Research*, *109*(24), 1–18. https://doi.org/10.1029/2004JD005093

Josse, B., Simon, P., & Peuch, V.-H. (2004). Radon global simulations with the multiscale chemistry and transport model MOCAGE. *Tellus B: Chemical and Physical Meteorology*, *56*(4), 339. https://doi.org/10.3402/tellusb.v56i4.16448

Kawamiya, M., Hajima, T., Tachiiri, K., Watanabe, S., & Yokohata, T. (2020). Two decades of Earth system modeling with an emphasis on model for interdisciplinary research on climate (MIROC). *Progress in Earth and Planetary Science*, *7*(1), 64. https://doi.org/10.1186/s40645-020-00369-5

Marsh, D. R., Mills, M. J., Kinnison, D. E., Lamarque, J. F., Calvo, N., & Polvani, L. M. (2013). Climate change from 1850 to 2005 simulated in CESM1(WACCM). *Journal of Climate*, *26*(19), 7372–7391. https://doi.org/10.1175/JCLI-D-12-00558.1

Molod, A., Takacs, L., Suarez, M., & Bacmeister, J. (2015). Development of the GEOS-5 atmospheric general circulation model: Evolution from MERRA to MERRA2. *Geoscientific Model Development*, *8*(5), 1339–1356. https://doi.org/10.5194/gmd-8-1339-2015

Morgenstern, O., Braesicke, P., O'Connor, F. M., Bushell, A. C., Johnson, C. E., Osprey, S. M., & Pyle, J. A. (2009). Evaluation of the new UKCA climate-composition model-part 1: The stratosphere. *Geoscientific Model Development*, *2*(1), 43–57. https://doi.org/10.5194/gmd-2-43-2009

Morgenstern, O., Zeng, G., Abraham, N. L., Telford, P. J., Braesicke, P., Pyle, J. A., et al. (2013). Impacts of climate change, ozone recovery, and increasing methane on surface ozone and the tropospheric oxidizing capacity. *Journal of Geophysical Research: Atmospheres*, *118*(2), 1028–1041. https://doi.org/10.1029/2012JD018382

O'Connor, F. M., Johnson, C. E., Morgenstern, O., Abraham, N. L., Braesicke, P., Dalvi, M., et al. (2014). Evaluation of the new UKCA climate-composition model-part 2: The troposphere. *Geoscientific Model Development*, *7*(1), 41–91. https://doi.org/10.5194/gmd-7-41-2014

Oman, L. D., Douglass, A. R., Ziemke, J. R., Rodriguez, J. M., Waugh, D. W., & Nielsen, J. E. (2013). The ozone response to ENSO in aura satellite measurements and a chemistry-climate simulation. *Journal of Geophysical Research: Atmospheres*, *118*(2), 965–976. https://doi.org/10.1029/2012JD018546

Oman, L. D., Ziemke, J. R., Douglass, A. R., Waugh, D. W., Lang, C., Rodriguez, J. M., & Nielsen, J. E. (2011). The response of tropical tropospheric ozone to ENSO. *Geophysical Research Letters*, *38*(13), 2–7. https://doi.org/10.1029/2011GL047865

Revell, L. E., Tummon, F., Stenke, A., Sukhodolov, T., Coulon, A., Rozanov, E., et al. (2015). Drivers of the tropospheric ozone budget throughout the 21st century under the medium-high climate scenario RCP 6.0. *Atmospheric Chemistry and Physics*, *15*(10), 5887–5902. https://doi.org/10.5194/acp-15-5887-2015

Scinocca, J. F., McFarlane, N. A., Lazare, M., Li, J., & Plummer, D. (2008). Technical note: The CCCma third generation AGCM and its extension into the middle atmosphere. *Atmospheric Chemistry and Physics*, *8*(23), 7055–7074. https://doi.org/10.5194/acp-8-7055-2008

Stenke, A., Schraner, M., Rozanov, E., Egorova, T., Luo, B., & Peter, T. (2013). The SOCOL version 3.0 chemistry-climate model: Description, evaluation, and implications from an advanced transport algorithm. *Geoscientific Model Development*, *6*(5), 1407–1427. https://doi.org/10.5194/gmd-6-1407-2013

Stone, K. A., Morgenstern, O., Karoly, D. J., Klekociuk, A. R., French, W. J., Abraham, N. L., & Schofield, R. (2016). Evaluation of the ACCESS - chemistry-climate model for the southern hemisphere. *Atmospheric Chemistry and Physics*, *16*(4), 2401–2415. https://doi.org/10.5194/acp-16-2401-2016

Sudo, K., & Akimoto, H. (2007). Global source attribution of tropospheric ozone: Long-range transport from various source regions. *Journal of Geophysical Research*, *112*(12), 1–21. https://doi.org/10.1029/2006JD007992

Sudo, K., Takahashi, M., Kurokawa, J. I., & Akimoto, H. (2002). CHASER: A global chemical model of the troposphere 1. Model description. *Journal of Geophysical Research*, *107*(17), ACH7-1–ACH7-20. https://doi.org/10.1029/2001JD001113

Sukhodolov, T., Egorova, T., Stenke, A., Ball, W. T., Brodowsky, C., Chiodo, G., et al. (2021). Atmosphere-ocean-aerosol-chemistry-climate model SOCOLv4.0: Description and evaluation. *Geoscientific Model Development*, *14*(9), 5525–5560. https://doi.org/10.5194/gmd-14-5525-2021

Tatebe, H., Ogura, T., Nitta, T., Komuro, Y., Ogochi, K., Takemura, T., et al. (2019). Description and basic evaluation of simulated mean state, internal variability, and climate sensitivity in MIROC6. *Geoscientific Model Development*, *12*(7), 2727–2765. https://doi.org/10.5194/gmd-12-2727-2019

Tian, W., & Chipperfield, M. P. (2005). A new coupled chemistry–climate model for the stratosphere: The importance of coupling for future O_3-climate predictions. *Quarterly Journal of the Royal Meteorological Society*, *131*(605), 281–303. https://doi.org/10.1256/qj.04.05

Walters, D. N., Williams, K. D., Boutle, I. A., Bushell, A. C., Edwards, J. M., Field, P. R., et al. (2014). The Met Office unified model global atmosphere 4.0 and JULES global land 4.0 configurations. *Geoscientific Model Development*, *7*(1), 361–386. https://doi.org/10.5194/gmd-7-361-2014

Watanabe, S., Hajima, T., Sudo, K., Nagashima, T., Takemura, T., Okajima, H., et al. (2011). MIROC-ESM 2010: Model description and basic results of CMIP5-20c3m experiments. *Geoscientific Model Development*, *4*(4), 845–872. https://doi.org/10.5194/gmd-4-845-2011

Yukimoto, S., Adachi, Y., Hosaka, M., Sakami, T., Yoshimura, H., Hirabara, M., et al. (2012). A new global climate model of the Meteorological Research Institute: MRI-CGCM3: -model description and basic performance-. *Journal of the Meteorological Society of Japan*, *90*(A), 23–64. https://doi.org/10.2151/jmsj.2012-A02

Yukimoto, S., Yoshimura, H., Hosaka, M., Sakami, T., Tsujino, H., Hirabara, M., et al. (2011). Meteorological Research Institute-Earth system model version 1 (MRI-ESM1). *Technical Reports of MRI*, *64*(64), 88. https://doi.org/10.11483/mritechrepo.64